Packaging of Large-scale Planar Lightwave Circuits

Kuniharu KATO, Motohaya Ishii and Yasuyuki Inoue

NTT Opto-electronics Laboratories
Tokai, Naka-gun, Ibaraki, 319-11, Japan
TEL:+81 29 287 7417
FAX:+81 29 287 7881
E-mail: kuni@iba.iecl.ntt.co.jp

Abstract

This paper describes the packaging of large-scale silica-based planar lightwave circuits (PLCs) , fabricated on Si substrates. They include arrayed-waveguide grating (AWG) multiplexers and star couplers with more than 32 channels, and optical matrix switches with a scale of 8 x 8 or greater. These devices all have a large channel-number or a large number of switch elements. There are various technological objectives and techniques related to large-scale PLCs which concern their optical, electrical, thermal, and mechanical characteristics. Sseveral techniques are presented in detail based on experimental results.

I. Introduction

Silica-based planar lightwave circuits (PLCs) [1,2] are key components in, for example, optically dense wavelength-division-multiplexing (WDM) systems, photonic switching systems, and subscriber networks, because of their excellent performance, potential for large-scale integration and reduced cost compared with discrete-type optical components.

There is no clear guideline for categorizing large-scale PLCs. However, this paper groups together N x N arrayed waveguide gratings (AWGs) and star couplers with more than 32 channels, and N x N optical matrix switches with a scale of 8 x 8 or greater, which all have a large channel-number or a large number of switch elements.

Packaging is an important technology in relation to a variety of practical PLC uses in indoor and outdoor environments. There are various technological objectives and techniques related to large-scale PLCs which concern their optical, electrical, thermal, and mechanical characteristics. The comparative importance of these techniques depends on the large-scale PLCs to be packaged.

This paper describes the packaging of large-scale silica-based PLCs. fabricated on Si substrates. Section II describes various PLCs and key technologies. Section III focuses on large-scale PLCs and packaging technology. Section IV and V deal with modules and possible future advances in packaging techniques for large-scale PLCs.

II. Silica-based PLCs and key technologies

Silica-based PLCs are fabricated on Si substrats by a combination of flame hydrolysis deposition (FHD) and reactive ion etching (RIE). In cross-section, the structure of a typical single-mode PLC has a squre waveguide core which is buried in a thick under- and overcladding layers. The total thickness of the glass layer on the Si substrate is around 60 μm . The parameters of typical SiO_2-GeO_2 waveguides [3,4] fabricated by the FHD/RIE method are listed in Table 1. The large-scale PLCs described in this paper mainly employ a high relative index difference Δ of 0.75 %. Figure 1 shows silica-based PLCs and the key technologies by which to achieve them. There are passive components, such as optical splitters, couplers, switches and WDM multiplexers, and active components such as hybrid integrated PLCs [5] and Er-doped PLCs [6] with an optical amplification function. Wavelength insensitive couplers (WINCs) [7] have been utilized in

Table 1 Parameters of typical PLC waveguides.

Waveguide type	Low Δ	Middle Δ	High Δ	Super high Δ
Refractive index difference Δ(%)	0.25	0.45	0.75	1.5 - 2
Core size (μm)	8x8	8x8	6x6 - 7x7	4x4 - 5x5
Propagation loss (dB/cm)	<0.1	0.017	0.035	0.07
Fiber coupling loss* (dB)	0.1	0.2	0.5	2 - 2.5
Minimum bending radius **(mm)	25	15	5	1 - 2

* Single-mode fiber used : 2a = 8.9 μm, Δ = 0.27 %, with index matching oil.
**Bending loss in a 90-degree arc waveguide is less than 0.1 dB at λ=1.55μm.

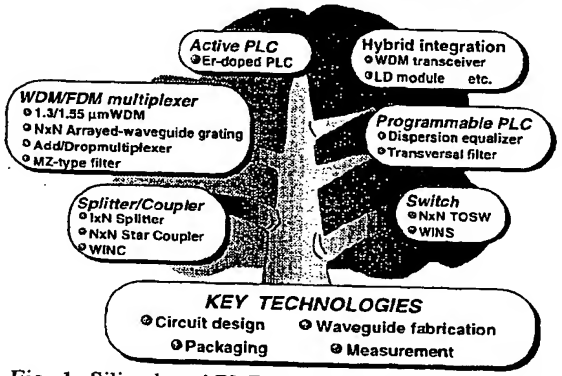

Fig. 1 Silica-based PLCs and the key technologies.

0-7803-3857-X/97 $4.00 ©1997 IEEE

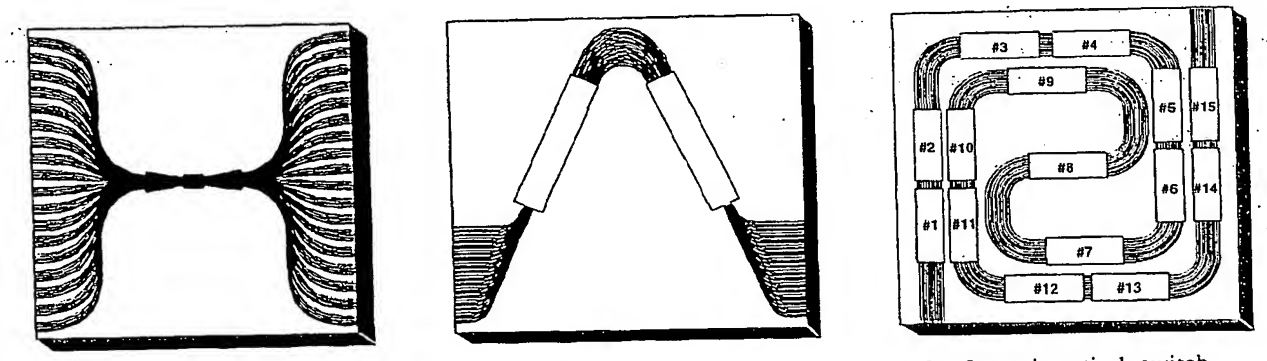

(a) 144 x 144 star coupler (b)64 x 64 AWG (c) 8 x 8 matrix optical switch.

Fig.2 Layout of large-scale PLCs dealt with in this paper.

commercial systems. Packaging is one of the key technologies, along with circuit design, waveguide fabrication and measurement, for realizing practical PLCs.

III. Large-scale PLCs and packaging technology

Figure 2 (a),(b) and (c) respectively, show the layout of a 144 x 144 star coupler [8], 64 x 64 AWG [9] and 8 x 8 optical matrix switch [10], which are the large-scale PLCs dealt with in this paper. The chip size depends on the layout and channel number, however, these PLCs are all larger than 6 x 3 cm^2.

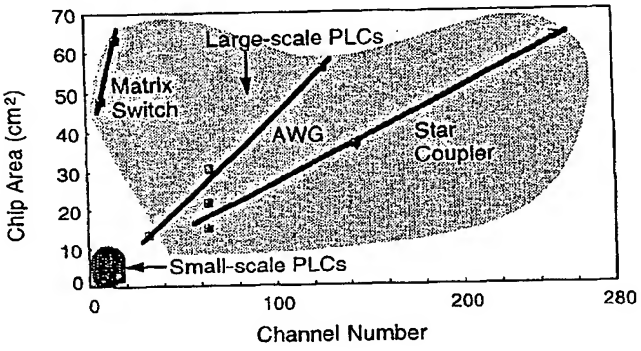

Fig. 3 Relationship between channel number and chip area.

Figure 3 shows the relationship between channel number, that is, input/output port number and chip area. Plots are shown for the above three types of large-scale PLC. These features depend on the waveguide layout as shown in Fig. 2. For example, the chip of a 144 x 144 star coupler is 6-cm square whereas the chip of an 8 x 8 matrix switch with 112 optical switch elements is 7.1 x 6.8 cm^2. Up to date, 256 x 256 star coupler [11], 128 x 128 AWG [12] and 16 x 16 optical matrix switch [13] have been demonstrated.

For comparison, the plots for small scale PLCs (2x8, 2x16 splitters, 4 channel WINCs and WDM transceiver) are shown in the bottom left of the figure. For example, the chip of the 2 x 8 splitter is 0.4 x 2.5 cm^2.

There are several problems to be dealt with in relation to packaging large-scale PLCs because of the large number of attached fibers, the large chip and their operation condisions. Figure 4 shows the developmental objectives and techniques for packaging large-scale PLCs in relation to their optical, electrical, thermal, and mechanical characteristics.

In terms of achieving low loss, fiber attachment techniques are important for all three large-scale PLCs ,in addition to low-waveguide propagation. A precise 32-fiber array [14] has been developed in order to reduce both the bonding and alignment cost.

A high return loss is required especially for applications to analog transmission systems. To this end, we have developed an angled fiber-array.

PLCs fabricated on Si substrates have the disadvantage of intrinsic birefringence due to internal stress. Birefringence control in order to realize polarization insensitivity is very important for AWGs because polarization dependent loss (PDL) becomes significant in PLCs that have a large diffraction order such as AWGs. We have developed a new control technique [15] for AWGs to simplify the phase control of the TE and TM modes.

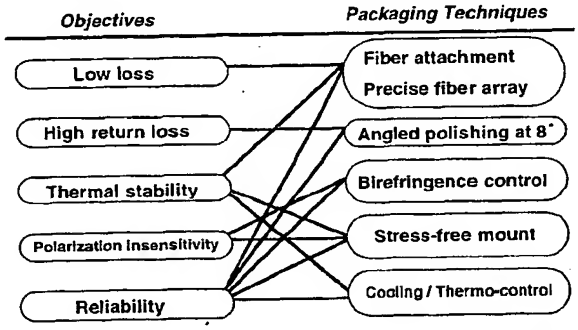

Fig. 4 Developmental objectives and the techniques for packaging large-scale PLCs.

The thermal stability of a PLC is affected by the PLC itself and external factors such as fiber attachment, and the PLC chip mount. The temperature of an AWG multiplexer

must be precisely controlled, since its transmission characteristics change readily if the AWG temperature changes, due to the thermal coefficient of the optical index. We have also developed a stress-free mount technique to avoid any degradation in the polarization insensitive transmission characteristics of due to partially induced stress when the PLC temperature is changed intentionally for tuning or unintentionally as a result of enviromental condition.

Heating power must be supplied to the 8 x 8 optical matrix switch because switching is accomplished by the thermo-optic effect of silica glass. It is therefore important to cool the 8 x 8 optical matrix switch in order to prevent its overheating.

We are studing the reliability of large-scale PLCs on the basis of 1 x 8 splitter packaging techniques. This is because these techniques provided excellent levels of performance and met Bellcore requirements [16].

Issues / Large-scale PLCs	Fiber attachment	Birefringence control	Stress-free mount	Cooling	Thermo-control
Star coupler 64 x 64, 144 x 144 256 x 256		—	—	—	—
Matrix switch 8 x 8, 16 x 16		—			—
AWG 32 x 32, 64 x 64 128 x 128				—	

: Importance

Fig.5 Comparative importance of packaging technologies for large-scale PLCs.

Figure 5 shows the comparative importance of packaging technologies for large-scale PLCs. Fiber attachment is an important technology in each case. Birefringence control, stress-free mounting and thermo-control are of particular importance for AWGs. Cooling is important for the matrix switch because it uses heating power for switching.

IV. Large-scale PLC modules

A. N x N star coupler modules

Optical N x N star couplers are important components in fiber optic communication networks, such as distribution, high-speed, and multiple-access networks, since they evenly divide in input signal among many receivers and make interconnection possible.

Figure 6 shows a photograph of a 64 x 64 star coupler module [9]. Both ends of the star coupler chip are fixed in metal frames and their endfaces are optically polished. Eight fibers are arrayed in precise glass V-grooves in a fiber holder at intervals of 250 μm and then fixed in a metal frame. Sixteen 8-fiber arrays were used for the star coupler module. We employed both adhesive bonding and YAG-laser welding for the star couplers in order to achieve a rigid connection. The adhesive was used to obtaine optical index matching between the waveguides of the star coupler and the fiber cores.

Figure 7 shows photograph of a packaged 64 x 64 star coupler module installed in a bookshelf type unit. The unit size is 28 x 32 x 20 cm^3. The 144 x 144 star coupler is also packaged in the same way. We used thirty-six 8-fiber arrays were used for the star coupler module. The 64 x 64 and 144 x 144 star coupler modules exhibit average insertion losses of 21.7 and 26.6 dB, respectively.

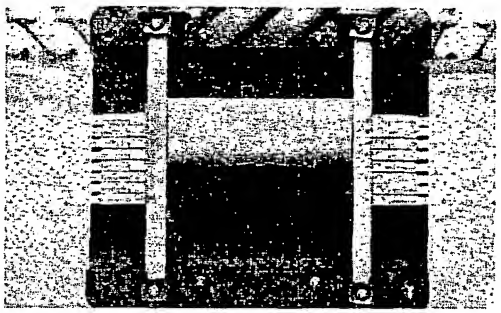

Fig. 6 Photograph of a 64 x 64 star coupler module.

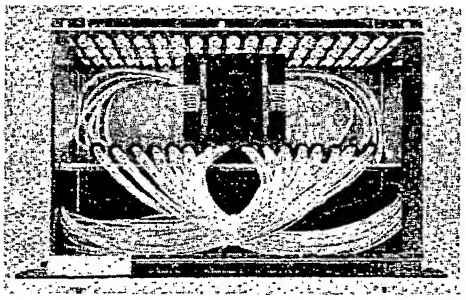

Fig. 7 Photographs of a packaged 64 x 64 star coupler module installed in a bookshelf type unit.

In terms of reducing both the bonding and alignment costs, it would be advantageous if more than 8 fibers cuold be connected presicely and simultanously to the large-scale N x N star couplers. One of main factors deciding the fiber number is the slight warping of the PLC. This warping is caused by the difference between the thermal expansion coefficients of silica glass and the silicon substrate and leads to excess connection loss. If a straight fiber array is connected to a PLC, it induces excess loss due to a deviation in the fiber-PLC connection. Multiple 32-fiber arrays have been developed in order to realize a low excess loss of 0.2 dB and a high fabrication yield.

The developed 32-fiber arrays (N = 22) with spacings of 250 μm exhibit pitch deviations of 0.41 μm (average) and 0.23 μm (standard deviation). These values indicate that a highly accurate 32-fiber array is successfully fabricated.

Figure 8 shows the layout of a star coupler [17] which

has four arrays composed of 32 channel waveguides. In the 64 x 64 star coupler connection process, both ends of the chip are bonded to glass plates using UV-curable adhesive in order to protect the chip endface and enhance the mechanical strength between the chip and the fiber array. The endfaces of the chip and the fiber arrays are polished at an angle of 8 degrees in order to suppress reflection at the endfaces. The chip and the 32-fiber array are aligned by launching a lightwave into two ports. After alignment, they are fixed in place using UV-curable adhesive.

Figure 9 shows a photograph of a 64 x 64 star coupler module with four 32-fiber arrays. By using this 32-fiber array, we successfully reduced the assembly time to one-fourth that needed with an 8-fiber array. The module exhibits an average insertion loss of 20.6 dB, including a connection loss of 0.4 dB for the two 32-fiber-array attachment points, and a return loss of higher than 50 dB which is the result of employing an angled fiber-array endface. These values indicate the excellent optical performance of the fabricated star coupler module. It also exhibited high stability with a loss deviation of less than 0.1 dB during temperature cycling from 75 to -40 ℃.

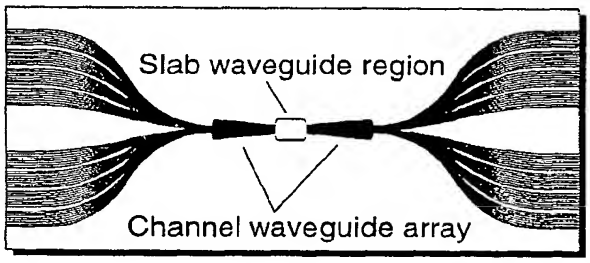

Fig. 8 Layout of a star coupler with four arrays composed of 32 channel waveguides.

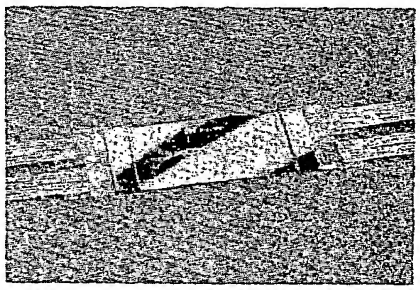

Fig. 9 Photograph of 64 x 64 star coupler module with four 32-fiber arrays.

B. N x N AWG module

N x N AWG multiplexers are key components in optically dense WDM systems, since they are capable of multi/demultiplexing N optical signals of different wavelengths.

Figure 10 shows a 32 x 32 AWG multiplexer with a thin-polyimide half-waveplate to control the birefringence of the PLC. It consists of plural input/output waveguides, two focusing slab waveguides and arrayed waveguides with a path difference ΔL. The input light is radiated to the first slab and then excites the arrayed channel waveguides. After propagating through the arrayed waveguides, the light beams are focused at output waveguides corresponding to the input light wavelength as a result of interference in the second slab waveguide.

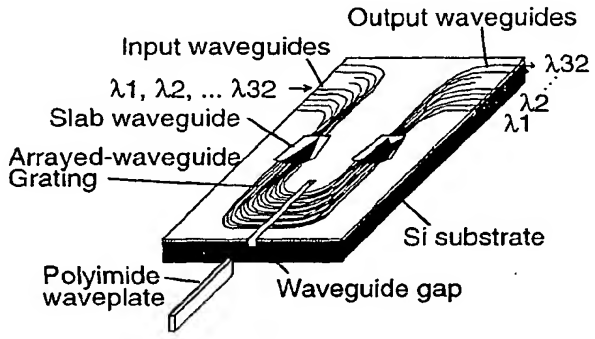

Fig. 10 32 x 32 AWG multiplexer.

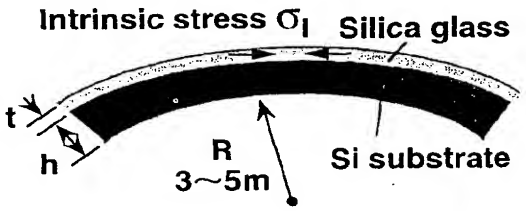

(a) Intrinsic stress caused by warping of the PLC chip.

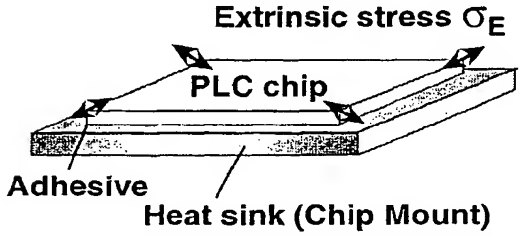

(b) Extrinsic stress caused by the structural materials of the PLC module.

Fig.11 Origins of birefringence in PLCs.

The use of birefringence control in order to realize polarization insensitivity is very important for AWG modules because polarization dependent loss (PDL) becomes significant in AWGs that have a large diffraction order. This birefringence B originates from both intrinsic stress σ_I and extrinsic stress σ_E. B is expressed as

$$B = n_{TM} - n_{TE} = B_0(\sigma_I) + B_E(\sigma_E) \qquad (1)$$

where n is the optical index of the waveguide, TM and TE

indicate respectively lightwaves polarized horizontally and perpendicularly to the PLC substrate. The intrinsic stress σ_I is caused by the warping of the PLC chip as shown in Fig.11 (a). This originates from the difference between the thermal expansion coefficients of silica glass and the silicon substrate and from the temperature drop of more than 1000 ℃ that occurs during the PLC fabrication process. The radius of the PLC warp is normally 3 to 5 meters. Consequently, PLC waveguides exhibit an intrinsic birefringence B_0 of 1 to 4 x 10^{-4} due to the photoelastic effect of silica glass under an intrinsic stress σ_I of 3 to 12 kg/mm^2.

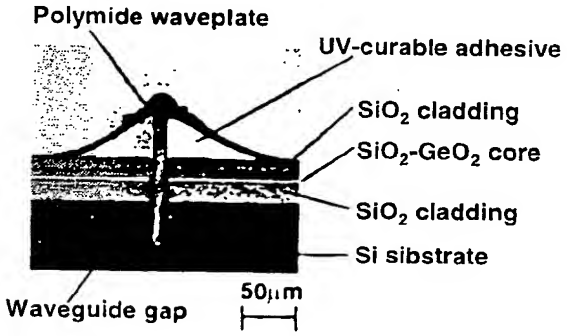

Fig. 12 Cross sectional photograph of the waveplate insertion region.

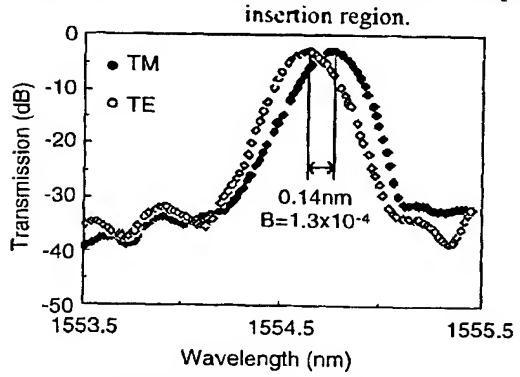

(a) without the polyimide waveplate.

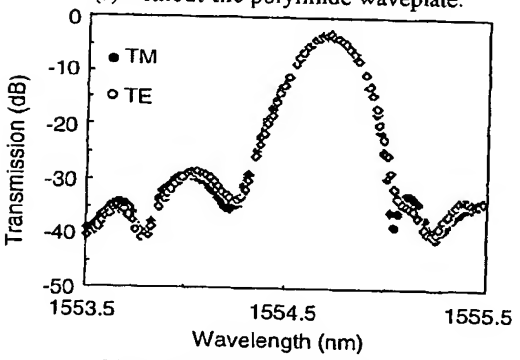

(b) with the polyimide waveplate.

Fig. 13 Transmission spectra of the AWG multiplexer.

We developed a new control technique [15] for AWGs in order to simplify the phase control of the TE and TM modes. This is a TE/TM mode conversion method in which a thin-polyimide half-waveplate is inserted in the center of an arrayed waveguide as shown in Fig. 10. Its principal axis is tilted at 45 degrees to the substrate so that it works as a TE/TM mode converter. Figure 12 shows a cross sectional photograph of the waveplate insertion region. A groove, 18 μm wide and 120 μm deep, is cut in the center of the arrayed waveguide grating. The thickness of the waveplate is 14.5 μm. Figure 13 (a) shows the transmission spectra without the polyimide waveplate. The waveguide birefringence is estimated to be 1.3×10^{-4} from the TE-TM wavelength shift of 0.14 nm. Figure 13 (b) shows the polarization insensitive characteristics with the polyimide waveplate. The discrepancy between the characteristics reveals that the waveplate has a low inserting loss of 0.4dB.

Another origin of birefringence is extrinsic stress caused by the difference between the thermal expansion coefficients of the PLC chip, adhesive, and heat sink materials as shown in Fig. 11 (b).

These materials compose a four-layer structure. The intrinsic stress σ_I changes very little in the temperature range of PLC operation. However, the extrinsic stress σ_E and birefringence have a likely temperature dependence and degrade the transmission characteristics when the PLC temperature is changed significantly for tuning.

The frequency tuning sensitivity in relation to temperature is 1.4 GHz (optical wavelength of 0.01nm)/K. This means that the development of a stress-free mount is a very important goal.

We calculated the extrinsic stress σ_E by using a three-dimensional computer simulation in order to realize a stress-free mount. Typical parameters, such as the thickness and thermal expansion coefficient, of the four-layer structure are listed in Table 2. PLC chips such as Mach-Zehnder inteferometers were conventionally mounted on a Cu heat sink by using a thermally conductive adhesive with a high Young's modulus. This was because frequency tuning was mainly carried out with a heater deposited on the PLC waveguide. We chose an adhesive with a low Young's modulus in order to realize a stress-free mount.

Figure 14 (a) shows a quarter model for the simulation and (b) and (c) show the calculated extrinsic stress profiles in the PLC when the temperature increment is 100 ℃ as examples. With the high Young's modulus adhesive over 100 kg/mm^2, the strain stress has a peak value of 5.4 kg/mm^2. On the other hand, when using a soft adhesive less than the Young's modulus of less than 0.5 kg/mm^2, no extrinsic stress occurs in the PLC.

Figure 15 shows the experimentally obtainedtemperature dependence of the birefringence of 10 GHz optical filters with conventional and stress-free mounts. The birefringence value is normalized at zero at a chip temperature of 0 ℃. This figure

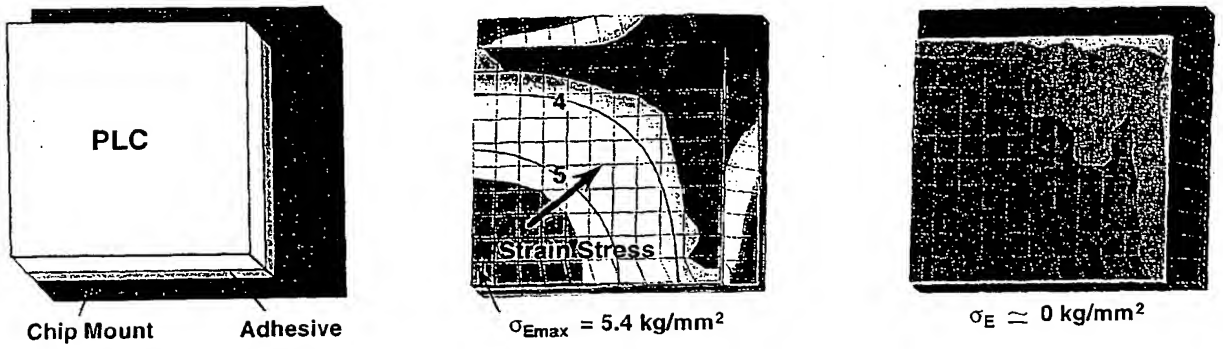

(a) Quarter model. (b) with high Young's modulus (c)with low Young's modulus.

Fig. 14 Simulation model and calculated extrinsic stress profiles in the PLC when the temperature increment is 100 ℃.

suggests that the birefringence of the PLC chip itself shows hardly any temperature dependence. However, the chip mounted with the high Young's modulus adhesive, that is a conventional mount, exhibits a high temperature dependence. On the other hand, the PLC chip with the stress-free mount shows similar characteristics to those of the chip itself. This result confirms the effectiveness of our stress-free mount.

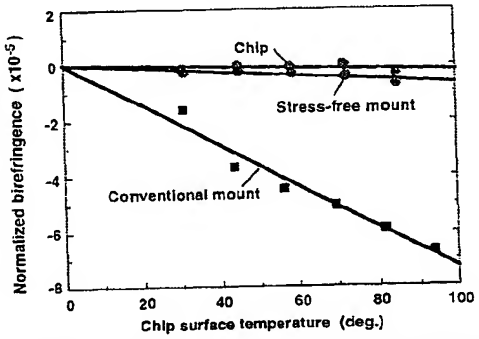

Fig. 15 Experimentally obtained temperature dependence of the birefringence.

Table 2 Typical thickness and thermal expansion coefficient parameters for the four- layer structure.

Layers	Stress-free mount	Conventional mount
PLC waveguide	Silica glass: t = 60 mm α = 0.13 ppm/K	
PLC substrate	Silicon: t = 1.0 mm α = 3.5 ppm/K	
Adhesive	Low Young's modulus t = 400 μm	High Young's modulu t = 400 μm
Heat sink (Chip mount)	Copper: t = 5.0 mm α = 16 ppm/K	

Figure 16 shows a photograph of a 32 x 32 AWG multiplexer. We use a Peltier device and a stress-free mount, respectively, for temperature control and to tune the optical characteristics. A 32-fiber array is also used for fiberattachment. Figure 17 shows the excellent transmission spectrum of a 32 x 32 AWG multiplexer with a channel spacing of 0.8 nm (100 GHz).

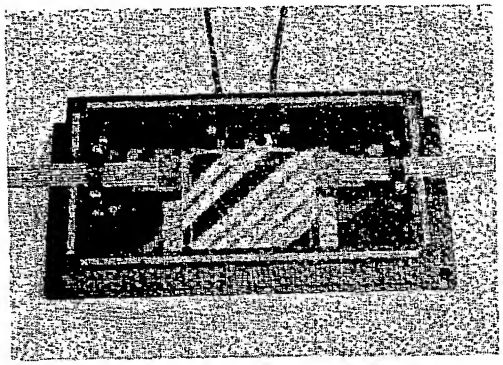

Fig. 16 Photograph of a 32 x 32 AWG multiplexer

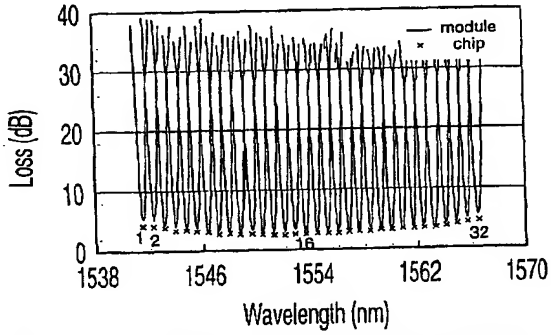

Fig. 17 Transmission spectrum of a 32 x 32 AWG multiplexer.

C. N x N optical matrix switch module

N x N space-division optical switches are indispensable for photonic switching systems, since they can switch optical signals directly without signal conversion and can trasmit analog and digital signals simultaneously.

Figure 18 shows the logical arrangement of a strictly nonblocking 8 X 8 optical matrix switch chip [10]. The switch consists of 64 active 2 x 2 switching elements which form a diamond shaped area and 48 loss balancers fixed in the

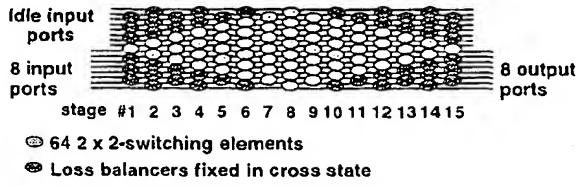

Fig. 18 Logical arrangement of a strictly nonblocking 8 x 8 optical matrix switch.

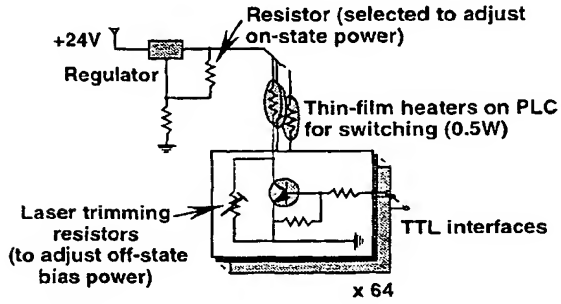

Fig. 19 Current-controllable driving circuits of 64-swiching elements.

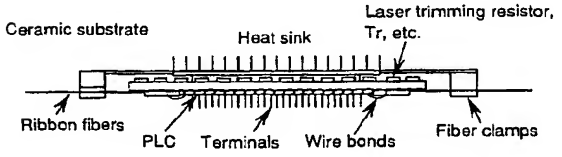

Fig. 20 Cross sectional view of 8 x 8 matrix switch module with hybrid integrated driving circuits on a 10 x10 cm^2 ceramic substrate.

cross state at the four corners. Each 2 x 2 switching element consists of an asymmetrical Mach-Zehnder interferometer (MZI) on which a thin-film heater is deposited, and an intersection. The 2 x 2 switching element is operated by electric power supplied to the heater because switching is accomplished by the thermo-optic (TO) effect of silica glass. Figure 2 (c) shows a practical waveguide layout for realizingthe logical arrangement. Fifteen switching unit stages are arranged on a 7.1 x 6.8 cm^2 chip. When the optical path is between the input and output ports, the switching element located at the optical crosspoint is turned on (on-state) by a heating power of about 0.5 W and the others are in the off state. Ideally, the off-state switching elements do not need any electric power. In practice, in order to realize a low crosstalk switch, it is necessary to supply a small power of about 0.05 W due to slight MZI fabrication errors. This optimum bias power varies from switch element to switch element. Therefore, 64 current-controllable driving circuits are required. Figure 19 shows the driving circuits of the 64-switching elements. Each off-state bias power can be adjusted with a laser trimming resistor. The on-state power of all 64 elements can be adjusted at one point by another laser trimming resistor. The driving circuits are designed to have TTL compatible interfaces. These driving circuits and the PLC chip are all mounted on a 10 x10 cm^2 ceramic substrate as shown in Fig. 20.

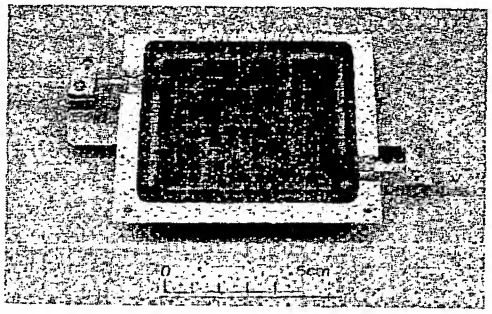

(a) PLC chip side.

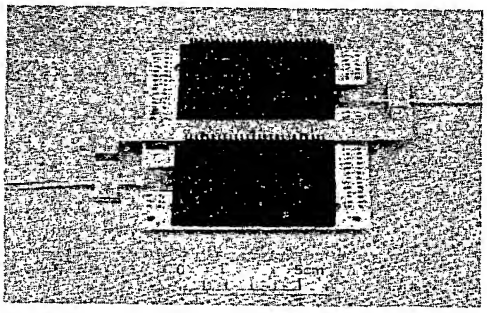

(b) opposite side.

Fig. 21 Photograph of the 8 x 8 matrix switch module with hybrid integrated driving circuits on a 10 x10 cm^2.

We fixed the PLC chip to the substrate by using thermally conductive adhesive with a low Young's modulus to reduce the thermal stress. 8-fiber and 16-fiber arrays are butted to the endfaces of the input and output ports, respectively. Fins for air cooling are attached to the opposite side of the PLC chip. Figure 21 (a) shows a photograph of the PLC chip side of the 8 x 8 matrix switch module. The hybrid integrated driving circuits and the fins for the heat sink are shown in Fig. 21 (b). The heating power of the switch elements and the power consumed by the driving circuits was 7 and 10 watts, respectively. The module exhibited a low insertion loss of 10 dB, a low crosstalk level of -25.9 dB, and had high mechanical and thermal stability.

V. Future advances in large-scale PLC packaging

We have developed a technique for fabricating PLCs with a refractive index difference Δn of greater than 1 % so that

might have a larger scale and higher-density integration. A 16 x 16 optical matrix switch [13] and 1 x 8 frequency-division multiplexer [18] with a Δn of 1.5 % have been fabricated. There is, however, a problem as regards the packaging of high-Δn waveguide and this is their poor coupling standard SMF's because of the optical mode-field mismatch between them. In order to solve this problem,we have developed mode-field conversion waveguides with thermally expanded cores (TEC waveguides) [19]. The original coupling loss of 2.0 dB was therby reduced to 0.9 dB. This excess loss of 0.9 dB was caused by misalignment between the TEC waveguides and the SM's and by the array pitch aberrations between the waveguides and the SMF array. It will be possible to realize a low coupling loss of less than 0.1 dB by overcoming these problems.

The combination of a large-scale PLC and a hybrid integration technique is expected to realize highly functional large-scale PLCs.

With regard to fiber attachment for large-scale PLCs, self-alignment technique using precise grooves integrated on PLCs is a promising technique for simplifying the coupling process between fibers and waveguides. Further advances in such packaging techniques as multiple-fiber connection and optical wiring will also contribute greatly to the successful development of large-scale PLCs.

VI. Conclusion

This paper has described packaging techniques for large-scale silica-based PLCs, fabricated on Si substrates. These techniques include fiber attachment, birefringence control, stress-free mount and cooling. It has also described packaging and characteristics of 64 x 64 and 144 x 144 star coupler, 32 x 32 AWG, and 8 x 8 optical matrix switch modules.

The packaging techniques we developed for the large-scale PLCs regarding their optical, electrical, thermal, and mechanical characteristics are as follows.

We designed a precise 32-fiber array to reduce the cost of bonding and alignment. We also construct an angled fiber-array in order to obtain a high return loss. We devised a thin polyimide half-waveplate for AWGs to control PLC birefringence. We developed a stress-free mount technique to avoid any degradation in the polarization insensitive transmission characteristics. We also developed 8 x 8 optical matrix switch modules with hybrid integrated driving circuits in which the matrix switch is cooled to prevent its overheating.

In the further, advances in the area of simplified fiber attachment and connection technology, optical wiring, and hybrid integration techniques will contribute greatly to the successful development of large-scale PLCs.

Acknowledgements

The authors wish to thank Drs. T. Miya, N. Takato, K. Okamoto, Y. Ohmori and M. Kawachi for their encouragement and helpful discussions. They would also like to thank I. Kitazawa for suggestion of 3D simulation and all members of the Photonic Component Laboratory for their contribution to this work.

References

[1] M. Kawachi, " Silica waveguides on silicon and their application to integrated-optic components," Optical and Quantum Electron.,vol.22, pp.391-416, 1990.

[2] M. Kawachi ,"Planar lightwave circuits for optical signal processing," Asia Pasific Microwave Conference '94, WS2-2, pp.39-44, 1994.

[3]Y. Hibino et al., "Propagation loss characteristics of long silica-based optical waveguides on 5 inch Si," Electron. Lett., vol.29, no.21, pp.1847-1848, 1993.

[4]Y. Hida et al., " 10 m long silica-based waveguide with a loss of 1.7 dB/m," IPR'95, Dana Point, CA, 1995.

[5]Y. Yamada et al., "Application of planar lightwave circuit platform to hybrid integrated optical WDM transmitter/receiver module'" Electron. Lett., vol.31, no.16, pp.1366-1367, 1995.

[6]T. Kitagawa et al. ,"Single-frequency Er-doped silica-based planar waveguide laser with integrated photo-imprinted Bragg refrectors," Electron. Lett., vol.30, no.16, pp.1311-1312, 1994.

[7]T. Oguchi et al., "Arrayed hybrid filter/coupler device for inservice fiber line testing," Electron. Lett., vol.29, no.20, pp.1786-1787, 1993.

[8] K. Kato et al. ," Packaging of large-scale integrated NxN star couplers," IEEE PTL., vol.4, no.3, pp.348-351, 1993.

[9]K. Okamoto et al., "Fabrication of 64 x 64 arrayed-waveguide grating multiplexer on silicon," Electron. Lett., vol.31, no.3, pp.184-186, 1995.

[10] R. Nagase et al., "Silica-based 8x8 optical matrix switch module with hybrid integrated driving circuits and its system application," IEEE J. LT., vol.12, no.9, pp.1631-1639, 1994.

[11] K. Okamoto et al., "Recent progress in silicon based integrated waveguide devices'" IPR'93, Palm Springs, CA, 1993.

[12] K. Okamoto, "Planar lightwave Circuits (PLCs)," International workshop on Photonic Network and Technologies, Lerici, Italy, 1996.

[13]M. Okuno et al., "Strictly nonblocking 16x16 matrix switch using silica-based planar lightwave circuits'" ECOC'94, PD, Firenze, 1994.

[14]M. Ishii et al., "Multiple 32-fiber array connection to silica waveguide on Si," IEEE PTL., vol.8, no.3 , pp.387-389, 1996.

[15] Y. Inoue et al., "Polarization mode converter with polimide half waveplate in silica-based planar lightwave circuits," IEEE PTL., vol.6, no.5 , pp.626-628, 1994.

[16] Y. Hibino et al., "High reliability silica-based PLC 1x8 splitters on Si," Electron. Lett., vol.30, no.8, pp.640-641, 1994.

[17] M. Ishii et al., "Multiple 32-fiber array connection to a silica waveguide on Si and its application to 64x64 PLC star couplers," IOOC'95, FA3-2, Hong-Kong, 1995.

[18]S. Suzuki et al., "High-density integrated planar lightwave circuits using SiO2-GeO2 waveguides with a high refractive index difference," IEEE J.LT., vol.12, no.5, pp.790-796, 1994.

[19]M. Yanagisawa et al., "Low-loss and large-tolerance fiber coupling of high-Δ silica waveguides by local mode-field conversion," IEEE PTL., vol.4, no.4 , pp.433-435, 1993.